



Since January 2020 Elsevier has created a COVID-19 resource centre with free information in English and Mandarin on the novel coronavirus COVID-19. The COVID-19 resource centre is hosted on Elsevier Connect, the company's public news and information website.

Elsevier hereby grants permission to make all its COVID-19-related research that is available on the COVID-19 resource centre - including this research content - immediately available in PubMed Central and other publicly funded repositories, such as the WHO COVID database with rights for unrestricted research re-use and analyses in any form or by any means with acknowledgement of the original source. These permissions are granted for free by Elsevier for as long as the COVID-19 resource centre remains active.



# PKR activation enhances replication of classical swine fever virus in PK-15 cells

Wen-Jun Liu, You-Tian Yang, Ming-Qiu Zhao, Xiao-Ying Dong, Hong-Chao Gou, Jing-Jing Pei, Jin-Ding Chen\*

*College of Veterinary Medicine, South China Agricultural University, 483 Wu Shan Road, Tian He District, Guangzhou 510642, China*



## ARTICLE INFO

### Article history:

Received 20 January 2015

Received in revised form 25 March 2015

Accepted 9 April 2015

Available online 18 April 2015

### Keywords:

CSFV

PKR

eIF2 $\alpha$

IFN- $\beta$

Innate immune

## ABSTRACT

Classical swine fever (CSF) is a highly contagious swine disease that is responsible for economic losses worldwide. Protein kinase R (PKR) is an important protein in the host viral response; however, the role of PKR in CSFV infection remains unknown. This issue was addressed in the present study using the PK-15 swine kidney cell line. We found that CSFV infection increased the phosphorylation of eukaryotic translation initiation factor (eIF2 $\alpha$ ) and its kinase PKR. However, the expression of viral proteins continued to increase. Furthermore, PKR overexpression enhanced CSFV replication, while PKR inhibition resulted in reduced CSFV replication and an increase in interferon (IFN) induction. In addition, PKR was responsible for eIF2 $\alpha$  phosphorylation in CSFV-infected cells. These results suggest that the activation of PKR during CSFV infection is beneficial to the virus. The virus is able to commandeer the host cell's translation machinery for viral protein synthesis while evading innate immune defenses.

© 2015 Elsevier B.V. All rights reserved.

## 1. Introduction

Classical swine fever (CSF), a swine disease classified as highly contagious by the World Organization for Animal Health, is characterized by high fever, multiple hemorrhage, leukopenia, neurological dysfunction, abortion, and high mortality (Moennig et al., 2013), and is the basis for considerable economic losses worldwide. The causative agent, CSF virus (CSFV), is an enveloped virus with a single-stranded positive-sense genomic RNA that is classified as a member of the Pestivirus genus within the Flaviviridae family (Becher et al., 2003). The CSFV genome contains 5' and 3' untranslated region (UTRs) and a single large open reading frame encoding four structural and eight nonstructural (NS) proteins (Sheng et al., 2012). An internal ribosome entry site (IRES) located in the 5' UTR regulates the translation of the viral genome (Fletcher and Jackson, 2002).

Translation is a key step for gene regulation in eukaryotic cells, especially when cells are stressed, such as during viral infection. Viral detection by cell sensors initiates a cascade of events that induces the transcription of IFN and other cytokines, shuts down protein synthesis and induces cell death in the cell's first line of defense to limit viral replication. PKR protein is IFN-induced

gene that is present in all vertebrates. It is activated by double-stranded RNA (dsRNA) which is often a by-product of virus replication. Recent studies have found that CSFV has evolved mechanisms to inhibit IFN production in infected cells, and preventing dsRNA-mediated apoptosis, which gives rise to long-term infections (Bauhofer et al., 2007; Ruggli et al., 2005, 2009; Seago et al., 2007, 2010); however, the role of PKR in CSFV infection has not been elucidated.

Eukaryotic translation initiation factor (eIF)2 is a key regulator of translation initiation. PKR is one of the four eIF2 $\alpha$  kinases – the others being general control non-derepressible 2, double-stranded RNA-activated protein kinase-like endoplasmic reticulum kinase, and heme-regulated inhibitor kinase – that phosphorylate eIF2 $\alpha$  in response to viral dsRNA, heme levels, misfolded proteins, and amino acid deprivation, respectively (Taylor et al., 2005). PKR binds to dsRNA and undergoes auto-phosphorylation, which activates the kinase that phosphorylates eIF2 $\alpha$  at Ser51, thereby inhibiting translation initiation and protein synthesis in various types of viral infection (Cole, 2007; Garcia et al., 2006). This constitutes the basic mechanism by which PKR exerts its antiviral activity on a wide spectrum of DNA and RNA viruses.

Some viruses can evade the antiviral function of PKR. Rotavirus infection can induce PKR activation, eIF2 $\alpha$  phosphorylation, and the modification of the cellular translation machinery while circumventing the host immune response. The phosphorylation of eIF2 $\alpha$  has been shown to block translation initiation of most

\* Corresponding author. Tel.: +86 20 8528 8017; fax: +86 20 8528 0245.

E-mail address: [jdchen@scau.edu.cn](mailto:jdchen@scau.edu.cn) (J.-D. Chen).

cellular proteins without affecting viral replication (Lopez and Arias, 2012; Rojas et al., 2010). In hepatitis C virus (HCV)-infected cells, PKR activation may be advantageous to the virus owing to reduced IFN production and consequent suppression of major histocompatibility complex I expression. In addition, PKR is responsible for the resistance of HCV to IFN treatment (Arnaud et al., 2010, 2011; Garaigorta and Chisari, 2009; Kang et al., 2014). In the Flaviviridae family, activated PKR was found to inhibit infection by West Nile virus (WNV) but not by dengue virus (Jiang et al., 2010).

Recent reports have shown that upon phosphorylation, eIF2 $\alpha$  can still associate with the IIId domain of the CSFV IRES, which delivers Met-tRNA to the P site of a 40S ribosomal subunit to form the 48S initiation complex (Friis et al., 2012; Hashem et al., 2013; Jackson et al., 2010; Locker et al., 2007; Pestova et al., 2008). Despite many studies, the function of PKR in CSFV infection is still unknown. In the present study, we investigated whether CSFV infection can activate PKR and eIF2 $\alpha$ , and examined the role of PKR in this process. The effect of PKR on CSFV replication and IFN induction was assessed by over-expressing or inhibiting PKR. Our results show that CSFV infection leads to activation of PKR and eIF2 $\alpha$  and enhances viral replication.

## 2. Materials and methods

### 2.1. Reagents

Primary antibodies against the following proteins were used in this study: PKR (BS3653), phospho-PKR $T^{446}$  (BS4789), and myxovirus resistance (MX)1 (BS6674) (all from BioWorld, Visalia, CA, USA); eIF2 $\alpha$  (SC-11386) and phospho-eIF2 $\alpha^{S51}$  (SC-12412) (both from Santa Cruz Biotechnology, Santa Cruz, CA, USA); CSFV E2 (WH303; Median Diagnostics, Chuncheon, Korea);  $\beta$ -actin (Beyotime, Beijing, China, AA128); and green fluorescent protein (GFP) (1533-1; Epitomics, Burlingame, CA, USA). Horseradish peroxidase-conjugated goat anti-rabbit (BS13278) and anti-mouse (BS12478) secondary antibodies were from BioWorld. Alexa Fluor 555-labeled donkey anti-rabbit (A0453) and Alexa Fluor 488-labeled goat anti-mouse (A0428) secondary antibodies were from Beyotime. 2-Aminopurine (2-AP; A2380) and poly(I:C) (P1530) were purchased from Sigma-Aldrich (St. Louis, MO, USA). The pEGFP-PKR and pEGFP-N1 vectors were prepared in our laboratory (Tian and Mathews, 2001). Monoclonal antibodies against the NS5A, NS3, and N $^{PRO}$  proteins of CSFV were provided by Dr. Xinglong Yu (Veterinary Department, Hunan Agricultural University, China). PKR and scrambled short hairpin (sh)RNA were designed by Cyagen Biosciences Inc. (Santa Clara, CA, USA). The PKR shRNA sequence 5'-GCA GAA CTT CTT CAC ATA TGT-3' was inserted into the pLenti X1-puro-shRNA-eGFP vector.

### 2.2. Cells and virus

The swine kidney cell line PK-15 (CCL-33; American Type Culture Collection, Manassas, VA, USA) was maintained in complete Dulbecco's Modified Eagle's Medium supplemented with 10% fetal bovine serum (FBS) and 1% antibiotics. Cells were incubated at 37 °C with 5% CO<sub>2</sub>. The CSFV Shimen strain used in this study was isolated from swine exhibiting typical CSF symptoms and was propagated in two cell cultures in medium containing 2% FBS, and then stored in our laboratory. Virus titers were determined using a monoclonal antibody against CSFV E2 as previously described (Pei et al., 2014). The multiplicity of infection (MOI) was calculated based on the virus titer. CSFV was inactivated by irradiating cells with ultraviolet (UV) light for 30 min at room temperature. The infectivity of UV-treated CSFV was confirmed by reverse transcription (RT)-PCR

to detect propagated virus, and the MOI was found to be the same as that of uninfected cells.

### 2.3. Viral infection

PK-15 cells were grown to ~80% confluence in cell culture plates and infected with CSFV at various MOIs. The mock-infected control was treated with phosphate-buffered saline (PBS). After 1 h, the inoculum was removed by aspiration. Cells were then washed twice with PBS and incubated in complete medium at 37 °C for various times until harvesting.

### 2.4. Western blotting

Cell monolayers were washed twice in PBS and incubated on ice with radioimmunoprecipitation lysis buffer (P0013B; Beyotime) containing 1 mM phenylmethylsulfonyl fluoride (ST506; Beyotime) for 10 min. Lysates were then centrifuged at 12,000 rpm for 20 min at 4 °C, and protein concentration was determined using a bicinchoninic acid assay kit (23227; Thermo Scientific, Waltham, MA, USA). Equal amounts of protein sample were boiled for 5 min in 5× sodium dodecyl sulfate polyacrylamide gel electrophoresis (SDS-PAGE) loading buffer. Proteins (20  $\mu$ g) were separated by 12% SDS-PAGE, electrotransferred to polyvinylidene fluoride membranes (IPFL00010; Merck Millipore, Billerica, MA, USA), and then blocked in 5% non-fat milk for 2 h at room temperature. Membranes were then incubated with primary antibodies at 4 °C overnight, washed three times for 10 min with PBS containing 0.5% Tween-20, and incubated with secondary antibody at 37 °C for 1 h. Protein bands were detected by enhanced chemiluminescence (P0018; Beyotime) and imaged using a CanoScan LiDE 100 scanner (Canon, Tokyo, Japan); band intensity was quantitated using Image J software (National Institutes of Health, Bethesda, MD, USA).

### 2.5. Confocal immunofluorescence microscopy

PK-15 cells were seeded on EZ SLIDES (Merck Millipore, PEZGS0816) and infected with CSFV at MOI of 1 or treated with PBS (mock-infected control). Cells were transfected with Lipofectamine 2000 (11668027; Life Technologies, Carlsbad, CA, USA) and 0.8  $\mu$ g poly(I:C) as negative and positive controls, respectively. After 24 h of incubation, cells were washed with PBS and fixed with 4% paraformaldehyde for 30 min at room temperature. Cell monolayers were permeabilized with 0.1% Triton X-100 for 30 min. Cells were then blocked with PBS containing 5% bovine serum albumin for 30 min at room temperature, and incubated for 1 h with rabbit polyclonal anti-eIF2 $\alpha$  (1:50) and mouse monoclonal anti-NS5A (1:100) antibodies in PBS at 37 °C, followed by a 1-h incubation in PBS containing Alexa Fluor 488 goat anti-mouse and Alexa Fluor 555 goat anti-rabbit secondary antibodies (1:200). Fluorescence was visualized using an LSM 780 confocal microscope (Zeiss, Jena, Germany).

The translocation of eIF2 $\alpha$  was determined as a ratio of nuclear to cytoplasmic localization of the protein. Quantification was performed using ImageJ software (National Institutes of Health; Bethesda, MD, USA). Images were acquired of three random fields from each sample. The cytoplasm and nuclear regions were determined by using ImageJ binary mask and image subtraction calculation. All samples in the same experiment were recorded with the same microscopic settings so that the images were comparable. Duplicate slides were made of each sample and three independent experiments were conducted (Noursadeghi et al., 2008; Zhu and Carver, 2012).

To assess the effects of PKR activation in CSFV-infected cells, PK-15 cells grown to ~70% confluence on EZ SLIDES were transfected with pEGFP-PKR plasmid using Lipofectamine 2000 reagent

as described below. After 24 h of incubation, immunocytochemical analysis was performed as described. Cells transfected with the empty vector (pEGFP-N1) served as the control groups. The efficiency of transfection and PKR protein expression were assessed by immunoblotting.

## 2.6. Biochemical intervention

For PKR inhibition experiments, cells grown to 80% confluence in 6-well culture plates were pretreated with 2-AP at concentrations of 0, 2.5, 5, 10, and 20 mM for 2 h prior to viral infection; adsorption was performed at 37 °C for 1 h. The inoculum was removed and washed twice with PBS, and cells were then incubated in fresh medium containing 2-AP at concentrations of 0, 2.5, 5, 10, and 20 mM. An equivalent volume of PBS was added to control cells. Based on these and published results (Knoetig et al., 2002), a concentration of 10 mM was used in subsequent experiments.

## 2.7. PKR over-expression and shRNA-mediated gene silencing

PK-15 cells were grown to 70% confluence in 6-well cell culture plates; 2 h before transfection, the cell culture medium was removed and replaced with 2 mL fresh medium containing 10% FBS. Cells were transfected with pEGFP-PKR or PLenti X1-puro-PKR shRNA-eGFP plasmid using Lipofectamine 2000 according to the manufacturer's protocol. Briefly, 2 µg DNA were resuspended in 150 µL serum-free OptiMEM medium while 10 µL Lipofectamine was diluted in 150 µL OptiMEM. The DNA and Lipofectamine solutions were combined at a 1:1 ratio and, after a 5-min incubation, added to the cells, which were cultured at 37 °C for 24 h. Following 1 h of CSFV adsorption, cells were incubated in fresh medium until cells or media were collected. The protein expression level and gene knockdown efficiency were evaluated by immunoblotting, and the empty (pEGFP-N1) or non-targeting shRNA vectors were used as negative controls for overexpression and knockdown experiments, respectively.

## 2.8. Real-time RT-PCR

Real-time quantitative (q)RT-PCR was used to detect CSFV and IFN-β RNA levels. The relative abundance of each target was calculated by normalizing to the level of glyceraldehyde-3-phosphate dehydrogenase (GAPDH). Total RNA was extracted from CSFV-infected cells using RNAiso Plus (9109; Takara Bio Inc., Otsu, Japan), and cDNA was synthesized using the PrimeScript RT Master Mix (RR036A; Takara Bio Inc.) according to the manufacturer's protocol. For CSFV-specific detection, the primer pair CCT GAG GAC CAA ACA CAT GTT G (CSFV1) and TGG TGG AAG TTG GTT GTG TCT G (CSFV2) – targeting a region corresponding to the NS5B gene – was used (Diaz et al., 1998). Primers for IFN-β and GAPDH were synthesized by Takara Bio Inc., and had the following sequences: TCG CTC TCC TGA TGT GTT TCT (IFN-β1) and AAA TTG CTG CTC CTT TGT TGG T (IFN-β2); and TGG AGT CCA CTG GTG TCT TCA C (GAPDH1) and TTC ACG CCC ATC ACA AAC A (GAPDH2). The qRT-PCR reaction was performed with SYBR Premix Ex Taq II (DRR081; Takara Bio Inc.) on an iQ5 iCycler detection system (Bio-Rad, Hercules, CA, USA) using previously described reaction conditions (Perez et al., 2011).

## 2.9. Quantification of IFN-β by enzyme-linked immunosorbent assay (ELISA)

PK-15 cells were seeded in 6-well plates and treated with 2-AP or shRNA and poly(I:C) (2 µg); 1 day later, cells were infected with the CSFV Shimen strain at an MOI of 1. At 24 h post-infection (hpi), cell culture supernatants were collected for analysis of IFN-β

protein level by ELISA (Cloud-Clone Corp., Houston, TX, USA) according to manufacturer's protocol.

## 2.10. Cell viability assay

Cell viability was evaluated with the Cell Counting Kit (CCK)-8 assay (C0037; Beyotime) according to the manufacturer's instructions. Briefly, cells were seeded in 96-well culture plates at a density of  $2 \times 10^3$  cells/well and cultured for 24 h at 37 °C. To assay the effects of 2-AP on cell proliferation, the culture medium was replaced with fresh medium containing 10 or 20 mM 2-AP or the equivalent volume of PBS for 48 h. To evaluate the effects of transfected plasmids on cell proliferation, the culture medium was replaced and plasmids were transfected as described for 48 h. A 10-µL volume of CCK-8 reagent was added to the cells for 1 h at 37 °C. The optical density was measured at 450 nm using a Model 680 microplate reader (Bio-Rad).

## 2.11. Statistical analysis

Data are expressed as the mean ± SEM and were analyzed by two-way analysis of variance using SPSS software version 17.0 (SPSS Inc., Chicago, IL, USA).  $P < 0.05$  was considered statistically significant.

## 3. Results

### 3.1. CSFV infection triggers PKR and eIF2α protein phosphorylation

Previous studies detected high levels of dsRNA in CSFV-infected cells (Bauhofer et al., 2005), while transfection of CSFV 5' UTR-Luc-3' UTR RNA induced the phosphorylation of eIF2α, which is downstream molecules of PKR (Hsu et al., 2014). However, it was not known whether PKR and eIF2α were activated in CSFV infection. The phosphorylation status of eIF2α and its kinase PKR during CSFV infection was assessed by infecting PK-15 cells with CSFV at various MOIs and analyzing cell extracts 24 hpi by Western blotting. The phosphorylation of eIF2α and PKR increased dose-dependently (Fig. 1A, lanes 1 and 5), and was detected as early as 24 hpi (Fig. 1B, lanes 1–6) upon CSFV infection (MOI = 1). CSFV NS3 protein level increased continuously upon eIF2α activation. To determine whether eIF2α and PKR activation was viral replication-dependent, cells were infected with UV-inactivated CSFV and eIF2α and PKR phosphorylation was assessed. In treated cells, eIF2α and PKR phosphorylation levels were close to the detection limit (Fig. 1A, lanes 6–10). These findings indicate that CSFV infection triggers the phosphorylation of PKR and eIF2α.

### 3.2. eIF2α is translocated from the nucleus to the cytoplasm in CSFV-infected cells

P-eIF2α was found redistributed to the cytoplasm from the nucleus under stress conditions (Kedersha et al., 2002). The localization of eIF2α in PK-15 cells and cells transfected with the PKR activator poly(I:C) or only lipo2000 transfected reagent was monitored by confocal microscopy. The eIF2α protein was mainly localized in the nucleus in uninfected cells, with limited cytoplasmic distribution (Fig. 2A and B); upon treatment with poly(I:C), nuclear eIF2α was translocated to the cytoplasm (Fig. 2A and B). In CSFV-infected PK-15 cells, eIF2α was excluded from the nucleus, as determined by immunostaining for CSFV NS5A proteins (Fig. 2A and B). Using the ImageJ/WCIF program with the intensity correlation analysis plugin, the colocalization rate was calculated. For eIF2α and NS5A protein the Pearson's Coefficient was 0.37 (0–0.5 indicates no colocalization and 0.5–1,

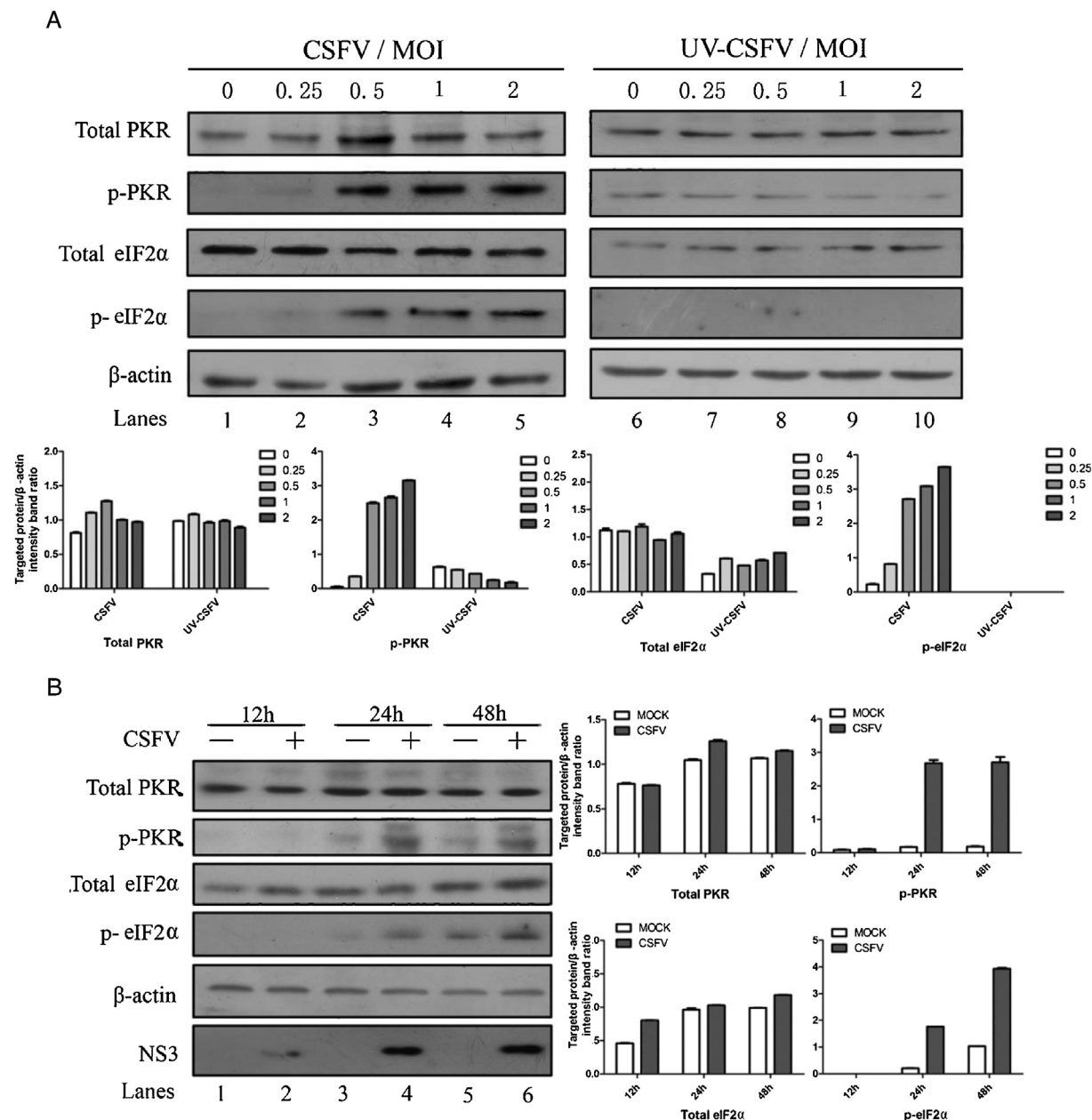


**Fig. 1.** CSFV infection triggers the phosphorylation of PKR and eIF2 $\alpha$  proteins. PK-15 cells were infected (+) or not (−) with CSFV shimen strain at MOI = 1. (A) Analysis by Western blotting of PKR, p-PKR, eIF2 $\alpha$ , p-eIF2 $\alpha$  and  $\beta$ -actin (loading control) in cellular extracts of CSFV infected or UV-CSFV infected in varying MOIs at 24 h after infection. The relative levels of the targeted proteins were estimated by densitometry, and the ratios were calculated relative to the  $\beta$ -actin control. Each sample represented a pool of three replicas. (B) At the indicated time points cellular extracts were prepared in RIPA buffer, their protein content was quantified by BCA and the accumulation of cellular PKR, p-PKR, eIF2 $\alpha$ , p-eIF2 $\alpha$ , NS3 and  $\beta$ -actin (loading control) proteins was analyzed by Western blotting. The relative levels of the targeted proteins were estimated by densitometry, and the ratios were calculated relative to the  $\beta$ -actin control. Each sample represented a pool of three replicas.

cocalocalization), which suggests that there is no cocalocalization between those two proteins. The Manders' overlap coefficient was 0.79 (0–0.6 indicates no cocalocalization and 0.6–1, cocalocalization), which indicate that there is partial overlap between those two proteins.

### 3.3. PKR over-expression stimulates, whereas PKR inhibition suppresses viral replication

To confirm the role of PKR in CSFV replication, pEGFP-PKR was transfected into cells. The mRNA of PKR itself can activate the enzyme, over-expression of PKR leads to its activation (Barber et al., 1993); Similar to what was observed upon CSFV

infection, eIF2 $\alpha$  was translocated to the cytoplasm (Fig. 3A), which was not observed in cells transfected with the control vector pEGFP-N1. Using the ImageJ/WCIF program with the intensity correlation analysis plugin, the cocalocalization rate was calculated. For eIF2 $\alpha$  and EGFP-PKR protein the Pearson's Coefficient was 0.795, which indicates that there is cocalocalization between those two proteins. In addition, eIF2 $\alpha$  phosphorylation level as well as N<sup>PRO</sup> and NS3 expression were enhanced in PKR-overexpressing cells (Fig. 3B), while intracellular CSFV RNA level (Fig. 3C) and virus titer (Fig. 3D) were also increased as compared to pEGFP-N1-transfected or mock-treated cells. These results indicate that PKR over-expression increases viral replication.

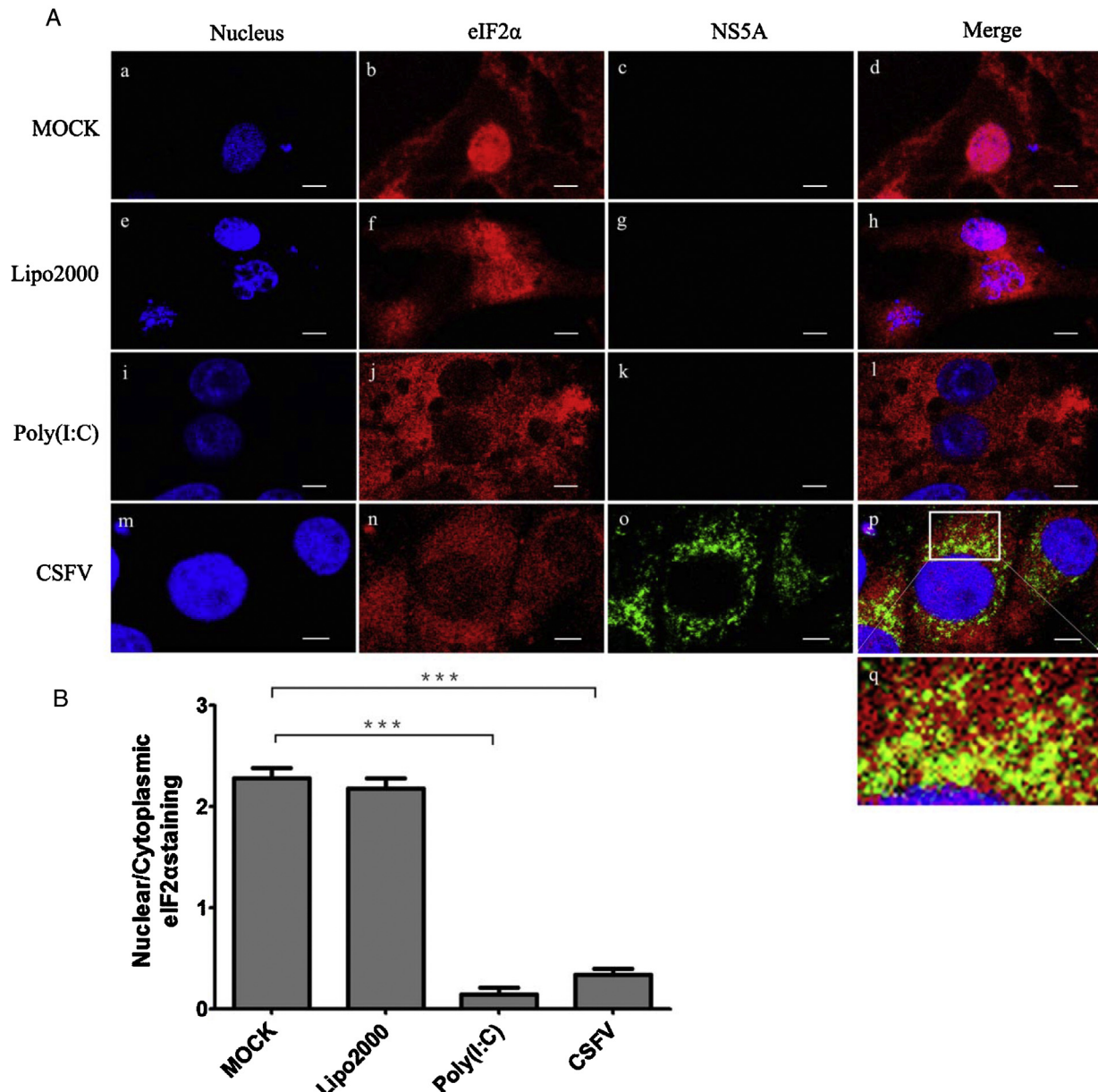


**Fig. 2.** Localization of eIF2 $\alpha$  in CSFV-infected cells. (A) Localization of eIF2 $\alpha$  in PK-15 cells under MOCK or lipo2000 or poly(I:C) treat or CSFV infect condition. poly(I:C)-treated PK-15 cells were transfected with 0.8  $\mu$ g poly(I:C) for 24 h. Lipo2000-treated PK-15 cells were transfected with transfect reagent only for 24 h. CSFV-infected cells were incubated for 24 h after inoculating with CSFV MOI = 1. Mock were treated with DMEM. eIF2 $\alpha$  and CSFV NS5A protein were visualized by immunocytochemistry using mouse monoclonal anti-CSFV NS5A protein and rabbit polyclonal anti-eIF2 $\alpha$  primary antibodies. Alexa Fluor 555-labeled Donkey Anti-Rabbit and Alexa Fluor 488-labeled Goat Anti-Mouse secondary antibodies were used as secondary antibodies. eIF2 $\alpha$  and CSFV NS5A proteins are shown in red and green, respectively. The cell nucleuses were counterstained with DAPI. The fluorescence signals were visualized by confocal immunofluorescence microscopy. In the images, the nucleus staining is shown in blue. Bars, 5  $\mu$ m. (B) Ratio of nuclear to cytoplasmic localization of the eIF2 $\alpha$ . All samples in the same experiment were recorded under the same microscopic settings to make pictures comparable to each other. The data represent the mean  $\pm$  SEM of 3 independent experiments. \*\*\*P<0.001. (For interpretation of the references to color in this figure legend, the reader is referred to the web version of this article.)

The inhibitor of PKR protein 2-AP acts as a competitive inhibitor of ATP during auto-phosphorylation following PKR activation (Knoetig et al., 2002; Hu and Conway, 1993; Lindquist et al., 2011). After testing different concentrations of 2-AP in CSFV-infected cells, it was found that the level of PKR and eIF2 $\alpha$  phosphorylation was lowest at 10 mM (Fig. 4A). To determine whether the pharmacological alteration of PKR activation by 2-AP affected the cell viability, evaluated the effects of 2-AP on cell viability with CCK-8 assay. Statistical analyses revealed no significant effects on the viability of cells treated with

10 mM 2-AP ( $P>0.05$ ) (Fig. S1A). This concentration was therefore used in subsequent experiments. Compared to untreated cells, NS5A expression level and CSFV titer were decreased in drug-treated cells (Fig. 4B). Furthermore, NS5A and NS3 protein and CSFV RNA expression were both reduced upon PKR inhibition combined with 2  $\mu$ g poly(I:C) treatment (Fig. 4C and D). These results suggest that PKR activation promotes CSFV replication.

Supplementary Fig. S1 related to this article can be found, in the online version, at <http://dx.doi.org/10.1016/j.virusres.2015.04.012>

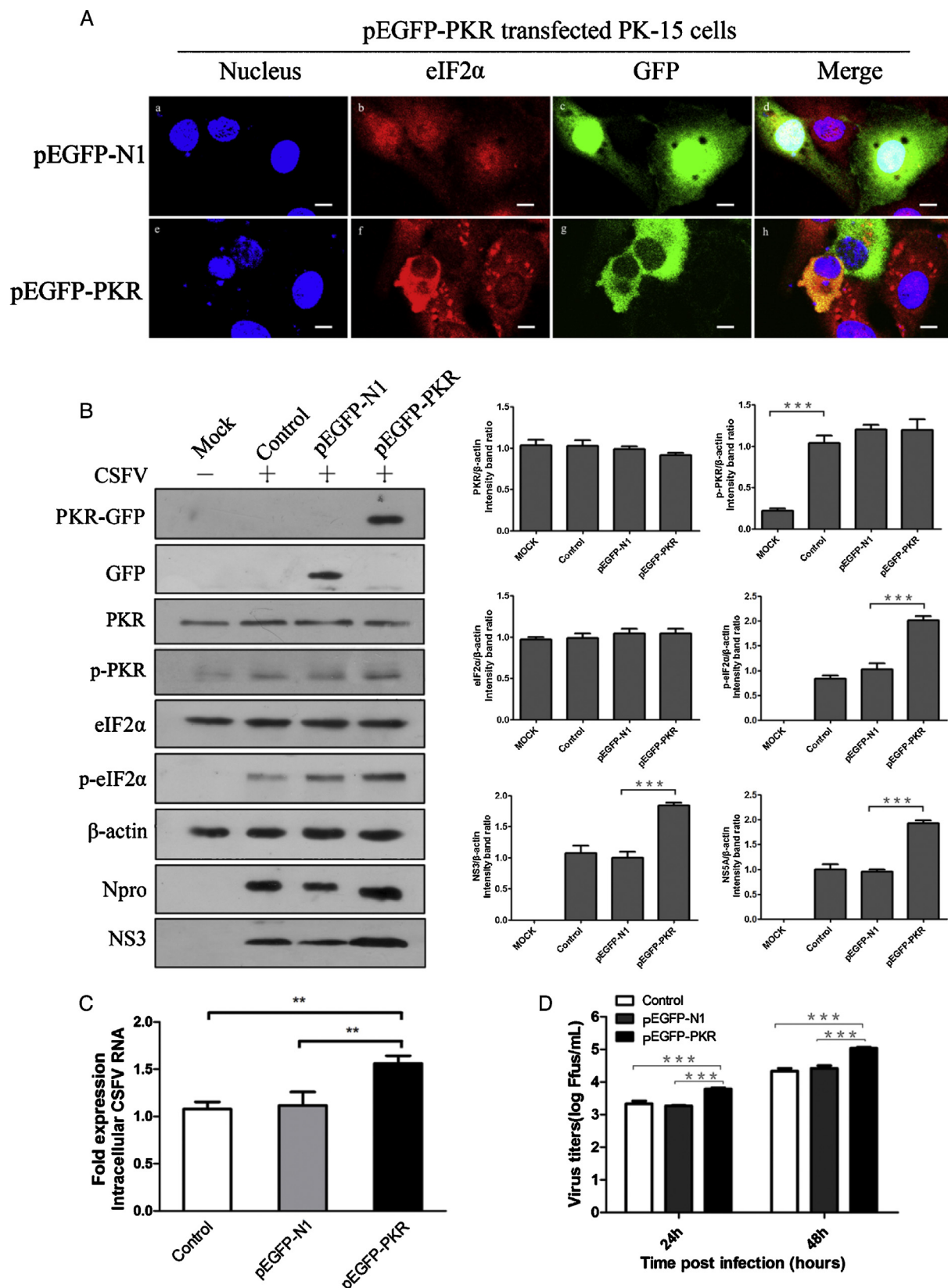


**Fig. 3.** Over-expression of PKR protein increase virus replication. (A) PK-15 cells were transfected with pEGFP-N1 or pEGFP-PKR expressing the PKR-GFP fusion protein. eiF2 $\alpha$  and PKR-GFP fusion protein and GFP protein were visualized by immunocytochemistry using rabbit polyclonal anti-eiF2 $\alpha$  primary antibodies. Alexa Fluor 555-labeled Donkey Anti-Rabbit secondary antibodies were used as secondary antibodies. eiF2 $\alpha$  and PKR-GFP/GFP proteins are shown in red and green, respectively. The cell nucleuses were counterstained with DAPI. The fluorescence signals were visualized by confocal immunofluorescence microscopy. In the images, the nucleus staining is shown in blue. Bars, 5  $\mu$ m. (B) PK-15 cells were transfected with pEGFP-N1 or pEGFP-PKR expressing the PKR-GFP fusion protein. Take PK-15 cells which transfected Lipo2000 as control. After 24 h of incubation, cells were infected with CSFV. Take uninfected cells as MOCK. Total cellular protein extracts of uninfected (—) and infected (+) cells were prepared in RIPA buffer was quantified by BCA. Analysis by Western blotting of PKR-GFP, GFP, PKR, p-PKR, eiF2 $\alpha$ , p-eiF2 $\alpha$ , N<sup>Pro</sup>, NS3 and  $\beta$ -actin (loading control) in cellular extracts.

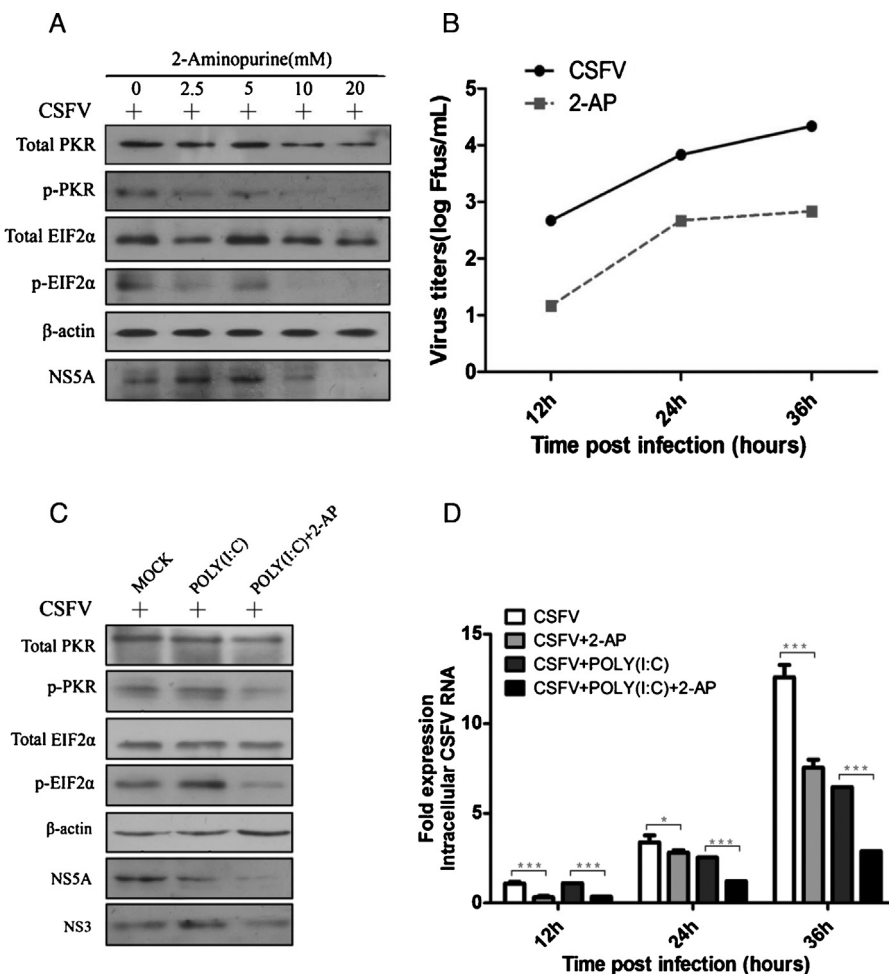


**Fig. 4.** Inhibition PKR with 2-Aminopurine (2-AP) decrease virus replication. (A) PK-15 cells treated with 2-AP at concentration of 0, 2.5, 5, 10, 20(mM/L) for 2 h prior to viral infection. Viral adsorption was performed at 37 °C for 1 h. The inoculum was removed and washed twice with PBS, and the cells were then incubated in fresh medium containing 2-Aminopurine at concentration of 0, 2.5, 5, 10, 20 (mM/L) respectively. Analysis by Western blotting of PKR, p-PKR, eIF2 $\alpha$ , p-eIF2 $\alpha$ , NS5A and  $\beta$ -actin (loading control) in cellular extracts. This experiment is representative of three independent experiments. (B) PK-15 cells treated with 2-AP (10 mM/L) were infected with CSFV. Take 2-AP untreated cells as control. At 12 hpi, 24 hpi, 36 hpi, virus titers were measured by endpoint dilution titrations by using the immunofluorescence assay. Results are expressed in units of FFus/mL. The data represent the mean  $\pm$  SEM of three independent experiments. (C) PK-15 cells transfected with 2  $\mu$ g poly(I:C) was infected with CSFV. Take poly(I: C) untreated cells as MOCK. Analysis by Western blotting of PKR, p-PKR, eIF2 $\alpha$ , p-eIF2 $\alpha$ , NS5A, NS3 and  $\beta$ -actin (loading control) in cellular extracts. This experiment is representative of three independent experiments. (D) Quantification of the intracellular CSFV RNA by RT-qPCR in total RNA isolated in 2-AP and poly(I:C) co-treated and only poly(I:C) treated cells. GAPDH mRNA quantification was used for normalization. Data are represented as mean  $\pm$  SEM;  $n = 3$ . This experiment is representative of 3 independent experiments. \* $P < 0.05$ ; \*\*\* $P < 0.001$ .

### 3.4. PKR depletion blocks eIF2 $\alpha$ phosphorylation and suppresses viral replication

To confirm the effects of PKR down-regulation on viral replication, endogenous PKR protein was depleted in PK-15 cells by shRNA knockdown. Similar to what was observed upon 2-AP treatment; PKR knockdown abolished eIF2 $\alpha$  phosphorylation and suppressed the expression of the viral proteins NS5A and NS3 and reduced viral RNA and titer as compared to control cells (Fig. 5A–G). In addition, viral replication was reduced in poly(I:C)-treated cells transfected with PKR shRNA (Fig. 5G). To confirm whether the transfected plasmids affected the capability of CSFV replication by changing the cell viability, same assay was taken. Statistical analyses revealed no

significant effects on the viability of cells ( $P > 0.05$ ) (Fig. S1B). Suggesting that PKR is responsible for eIF2 $\alpha$  phosphorylation during CSFV infection and is beneficial for viral replication.

### 3.5. PKR depletion increase IFN- $\beta$ , and enhances the antiviral effect of IFN

CSFV-infected PK-15 cells exhibited low levels of IFN- $\beta$  expression; a corresponding increase in IFN- $\beta$  mRNA expression was observed in poly(I:C)-treated cells. IFN- $\beta$  induction was increased by PKR knockdown at early stages of infection, attaining the same level as control cells at 48 hpi. (Fig. 6A and B). To confirm the early increase in IFN production in PKR-depleted cells, IFN- $\beta$  secretion

Each sample represented a pool of three replicas. (C) PK-15 cells were transfected and infected as in (B). Quantification of the intracellular CSFV RNA by RT-qPCR in total RNA isolated in cells. GAPDH mRNA quantification was used for normalization. Data are represented as mean  $\pm$  SEM;  $n = 3$ . This experiment is representative of three independent experiments. \*\* $P < 0.01$ . (D) PK-15 cells were transfected and infected as in (B and C). At 24 hpi and 48 hpi, virus titers were measured by endpoint dilution titrations by using the immunofluorescence assay described in Section 2. Results are expressed in units of FFus/mL. The data represent the mean  $\pm$  SEM of three independent experiments. \*\*\* $P < 0.001$ . (For interpretation of the references to color in this figure legend, the reader is referred to the web version of this article.)

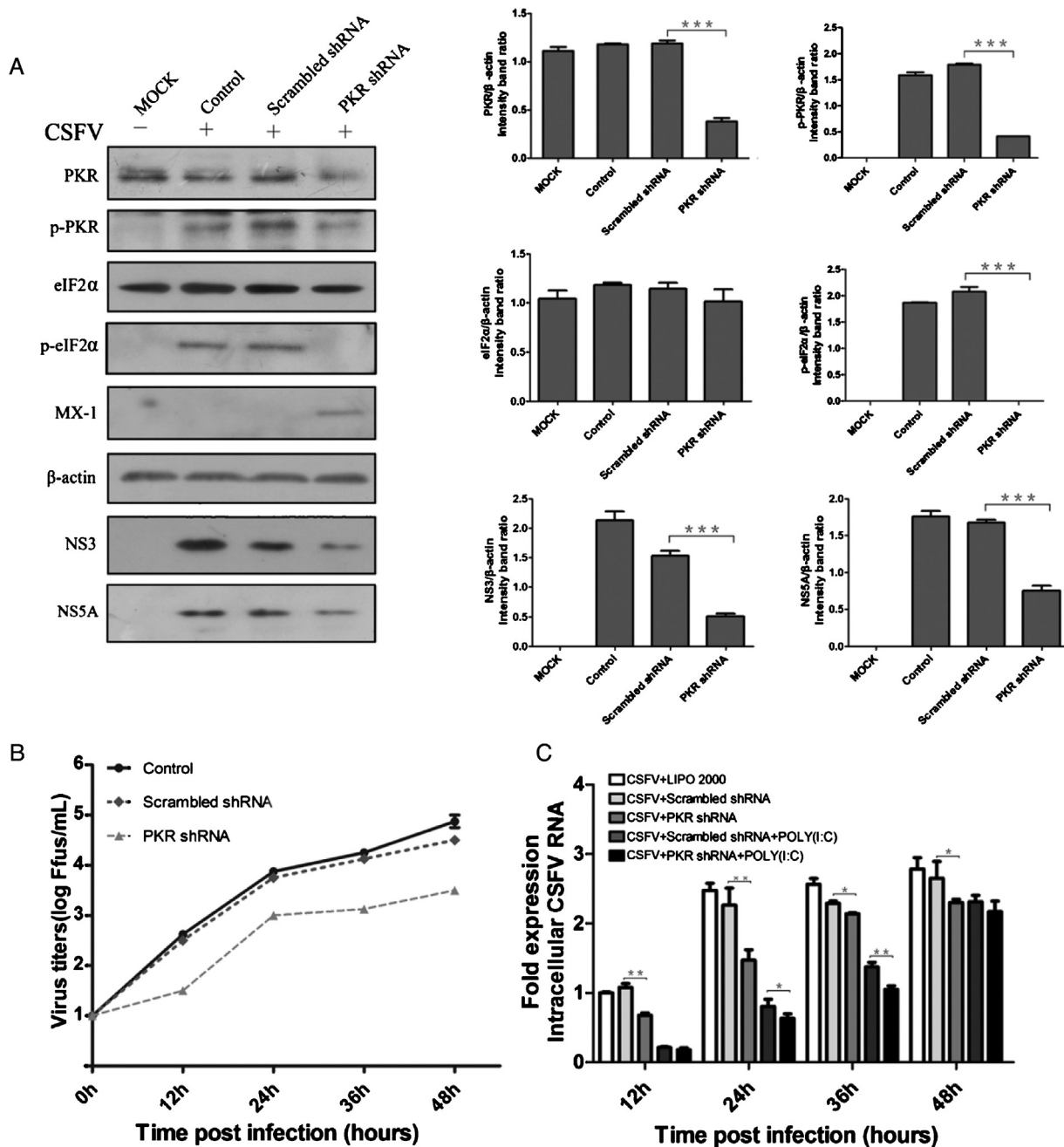


**Fig. 5.** Down-regulation of PKR by shRNA decrease virus replication. (A) Analysis by Western blotting of PKR, p-PKR, eIF2 $\alpha$ , p-eIF2 $\alpha$ , MX1, NS3, NS5A and  $\beta$ -actin (loading control) in cellular extracts of PK-15 cells transfected with PKR shRNA or Scrambled shRNA. Take PK-15 cells transfected with lipo2000 as control. Take CSFV uninfected PK-15 cells as MOCK. The intensity band ratios of the targeted proteins were estimated by densitometry, and the ratios were calculated relative to the  $\beta$ -actin control. This experiment is representative of 3 independent experiments. \*\* $P$ <0.01; \*\*\* $P$ <0.001. (B) PK-15 cells were transfected and infected as in (A). At 0 hpi, 12 hpi, 24 hpi, 36 hpi, 48 hpi virus titers were measured by endpoint dilution titrations by using the immunofluorescence assay. Results are expressed in units of FFus/mL. The data represent the mean  $\pm$  SEM of three independent experiments. (C) Quantification of the intracellular CSFV RNA by RT-qPCR in total RNA isolated in PK-15 cells transfected with PKR shRNA or Scrambled shRNA. Take PK-15 cells transfected with lipo2000 as control. GAPDH mRNA quantification was used for normalization. Data are represented as mean  $\pm$  SEM;  $n$ =3. This experiment is representative of three independent experiments. \* $P$ <0.05; \*\* $P$ <0.01; \*\*\* $P$ <0.001.

was measured 24 hpi under different treatment conditions. IFN- $\beta$  levels were elevated in cultures of 2-AP- and PKR shRNA-treated cells, and was further increased by co-treatment with poly(I:C) (Fig. 6C and D). PKR deficiency also stimulated the production of the IFN effector MX1 (Fig. 5A), which is not expressed in CSFV-infected cells and strongly inhibits CSFV replication (He et al., 2014). Taken together, these results indicate that PKR depletion not only increases induction but also enhances the antiviral effects of IFN- $\beta$ .

#### 4. Discussion

In the course of evolution, viruses have acquired numerous mechanisms to evade or subvert key elements of the host viral response. eIF2 $\alpha$  mediated translational control is the most important antiviral mechanism of PKR. The cap-dependent mechanism of translation initiation requires multiple eIFs and consists of two stages: the formation of the 48S initiation complex – for which eIF2 is required – and subsequent incorporation of the 60S

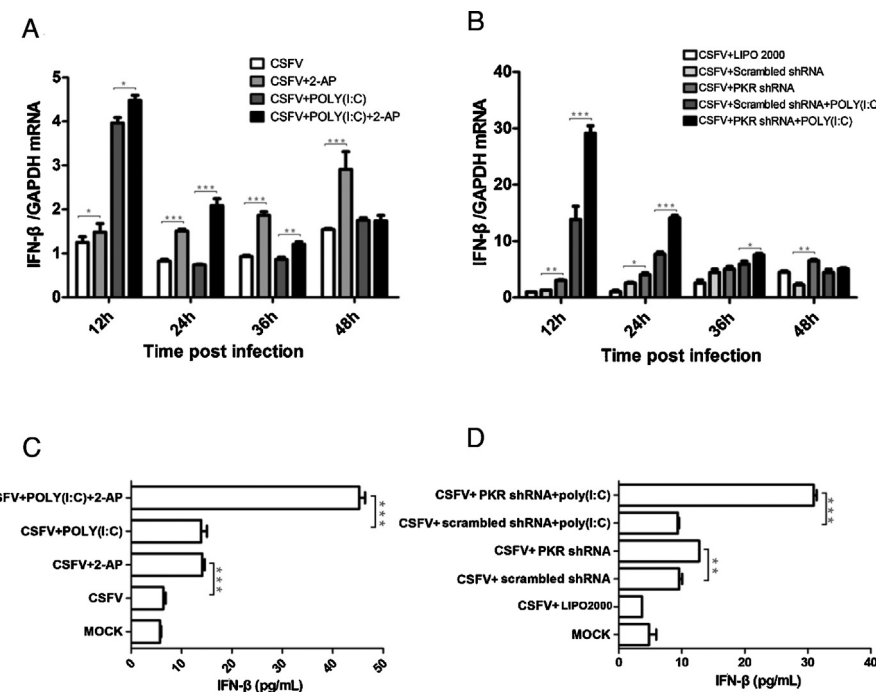


**Fig. 6.** Down-regulation of PKR increases IFN- $\beta$  induction. (A) PK-15 cells were first transfected with 2  $\mu$ g poly(I:C). 24 h post transfection, the cells were treated with 2-AP and then infected with CSFV at MOI of 1. At the indicated times, cells were processed for RNA extraction. Quantification of the intracellular IFN- $\beta$  mRNA by RT-qPCR in total RNA isolated in cells. GAPDH mRNA quantification was used for normalization. Data are represented as Mean  $\pm$  SEM;  $n = 3$ . This experiment is representative of three independent experiments. \* $P < 0.05$ ; \*\* $P < 0.01$ ; \*\*\* $P < 0.001$ . (B) PK-15 cells were first transfected with scrambled shRNA or PKR shRNA and co-transfected with poly(I:C). 24 h post transfection; the cells were infected with CSFV at MOI of 1. At the indicated times, cells were processed for RNA extraction. Quantification of the intracellular IFN- $\beta$  mRNA by RT-qPCR in total RNA isolated in cells. GAPDH mRNA quantification was used for normalization. Data are represented as mean  $\pm$  SEM;  $n = 3$ . This experiment is representative of 3 independent experiments. \* $P < 0.05$ ; \*\* $P < 0.01$ ; \*\*\* $P < 0.001$ . Cells were treated 2-AP (C) or shRNA (D) and poly(I:C) infected with CSFV at MOI of 1. At 24 hpi, cell culture supernatants were collected to analyze the protein expression of IFN- $\beta$  by ELISA. The experiment was repeated three times and the figure shows a representative experiment. Data is expressed as mean  $\pm$  SD. An asterisk indicates a statistically significant difference from uninfected cells, \*\* $P < 0.01$  and \*\*\* $P < 0.001$ .

subunit. When the  $\alpha$  subunit of the eIF2 is phosphorylated, eIF2-GDP does not recycle to eIF2-GTP and cellular translation is inhibited (Pestova et al., 2008; Sarnow, 2003). To overcome the inhibitory effects of eIF2 $\alpha$  phosphorylation, viruses either inhibit the activation of the eIF2 $\alpha$  kinases, e.g., adenovirus and hepatitis C virus (Gale et al., 1998; Schneider et al., 1985), or enhance the dephosphorylation rate of eIF2 $\alpha$ , e.g., herpes simplex 1 virus and coronavirus (He et al., 1997; Wang et al., 2009). However, in some cases, viral protein synthesis can proceed under conditions of eIF2 $\alpha$  phosphorylated as has been observed for HCV and rotaviruses. CSFV belongs to this last group. Interestingly, CSFV has a highly structured IRES that can associate with phosphorylated eIF2 $\alpha$  and deliver Met-tRNA to the P site of a 40S ribosomal subunit to form the 48S initiation complex (Friis et al., 2012; Hashem et al., 2013; Jackson et al., 2010; Locker et al., 2007; Pestova et al., 2008).

In this work, we found that PKR and eIF2 $\alpha$  phosphorylation was enhanced and eIF2 $\alpha$  was shuttled from the nucleus to the cytoplasm in CSFV-infected cells. However, the expression of viral proteins increased, suggesting that viral protein synthesis was insensitive to the inhibitory effects of phosphorylated eIF2 $\alpha$ . It was observed that the localization of eIF2 $\alpha$  and viral NS5A proteins partially overlapped. NS5A is an essential component of the viral RNA replication machinery, interacting with the 3' UTR of viral RNA and regulating its synthesis (Sheng et al., 2012). It is therefore possible that cytoplasmic eIF2 $\alpha$  is involved in the translation of CSFV RNA during infection. Consistent with these results, CSFV replication was enhanced in PKR over-expressing-cells, as evidenced by virus titer and increased viral RNA and protein levels. Conversely, PKR inhibition by 2-AP or shRNA decreased CSFV replication. PKR activation induces nuclear factor (NF)- $\kappa$ B translocation which in turns increases IFN- $\beta$  production (Gil et al., 1999; Stewart et al., 2003).

PKR is activated in CSFV-infected PK-15 cells while IFN transcription was unaltered. In addition, CSFV failed to activate NF- $\kappa$ B both *in vivo* and *in vitro* (Chen et al., 2012a,b). While inhibiting of PKR enhanced IFN expression, likely because PKR reduction decreased CSFV replication, thereby alleviating the inhibition of IFN induction. In this study, PKR was found to mediate CSFV-induced eIF2 $\alpha$  phosphorylation, since this was blocked by PKR depletion. Conversely, PKR activation promoted CSFV replication. MX1, an IFN-induced antiviral protein, strongly inhibited CSFV replication while it is not normally expressed in CSFV-infected cells (He et al., 2014). Suppressing PKR restored MX1 expression. These results suggest that CSFV infection triggers PKR and eIF2 $\alpha$  phosphorylation, which inhibits cellular protein synthesis, disrupts the host innate immune response, and ultimately enhances viral replication and reduces IFN- $\beta$  induction.

PKR has multiple functions, including the activation of NF- $\kappa$ B (Kumar et al., 1997) and p38 mitogen-associated protein kinase (Silva et al., 2004), modulation of the insulin pathway (Nakamura et al., 2010), apoptosis, autophagy (Talloczy et al., 2002), and activation of the inflammasome (Kang and Tang, 2012). Thus, there may be other mechanisms underlying the effect of PKR on CSFV replication. For instance, PKR also induces autophagy, which promotes CSFV replication (Pei et al., 2014). We found that PKR depletion inhibited CSFV induced autophagy (data not shown). On the other hand, viral components may have the capacity to regulate PKR: HCV NS5A interacts directly with PKR, which regulates HCV replication in conjunction with the HCV IRES (Gale et al., 1998; He et al., 2001; Toroney et al., 2010). In addition, Japanese encephalitis virus NS2A had been shown to block PKR (Tu et al., 2012), while PKR is not activated in WNV-infected rodent cells (Elbahesh et al., 2011). Whether similar

mechanisms exist in CSFV will be the subject of future investigations.

In summary, this study demonstrated that CSFV strongly induces PKR and eIF2 $\alpha$  phosphorylation, but was resistant to translational inhibition by eIF2 $\alpha$ . PKR over-expression enhanced CSFV replication, while PKR inhibition resulted in reduced CSFV replication. Moreover, PKR depletion enhanced the expression of IFN and consequently increased the expression of the IFN-induced antiviral effector protein MX1. These results indicate that CSFV utilizes PKR/eIF2 $\alpha$  signaling pathway enhances survival while evading the host immune response. These findings can explain why CSFV infection is persistent and characterized by low IFN levels.

## Acknowledgments

We are grateful to Dr Xinglong Yu of Hunan Agricultural University for providing the generous gifts of anti-NS5A, anti-NS3 and anti-N<sup>pro</sup> antibody.

This work was supported by the National Natural Science Foundation of China (Nos. U140526, 31472200 and 31172321), the Special Fund for Agro-Scientific Research in the Public Interest (No. 201203056).

## References

- Arnaud, N., Dabo, S., Akazawa, D., Fukasawa, M., Shinkai-Ouchi, F., Hugon, J., Wakita, T., Meurs, E.F., 2011. Hepatitis C virus reveals a novel early control in acute immune response. *PLoS Pathog.* 7 (10), e1002289.
- Arnaud, N., Dabo, S., Maillard, P., Budkowska, A., Kalliamvakou, K.I., Mavromara, P., Garcin, D., Hugon, J., Gatignol, A., Akazawa, D., Wakita, T., Meurs, E.F., 2010. Hepatitis C virus controls interferon production through PKR activation. *PLoS ONE* 5, e10575.
- Barber, G.N., Wambach, M., Wong, M.L., Dever, T.E., Hinnebusch, A.G., Katze, M.G., 1993. Translational regulation by the interferon-induced double-stranded-RNA-activated 68-kDa protein kinase. *Proc. Natl. Acad. Sci. U. S. A.* 90 (10), 4621–4625.
- Bauhofer, O., Summerfield, A., McCullough, K.C., Ruggli, N., 2005. Role of double-stranded RNA and N<sup>pro</sup> of classical swine fever virus in the activation of monocyte-derived dendritic cells. *Virology* 343 (1), 93–105.
- Bauhofer, O., Summerfield, A., Sakoda, Y., Tratschin, J.D., Hofmann, M.A., Ruggli, N., 2007. Classical swine fever virus N<sup>pro</sup> interacts with interferon regulatory factor 3 and induces its proteasomal degradation. *J. Virol.* 81 (7), 3087–3096.
- Becher, P., Avalos, R.R., Orlich, M., Cedillo, R.S., Konig, M., Schweizer, M., Stalder, H., Schirrmeier, H., Thiel, H.J., 2003. Genetic and antigenic characterization of novel pestivirus genotypes: implications for classification. *Virology* 311 (1), 96–104.
- Chen, L.J., Dong, X.Y., Shen, H.Y., Zhao, M.Q., Ju, C.M., Yi, L., Zhang, X.T., Kang, Y.M., Chen, J.D., 2012a. Classical swine fever virus suppresses maturation and modulates functions of monocyte-derived dendritic cells without activating nuclear factor kappa B. *Res. Vet. Sci.* 93 (1), 529–537.
- Chen, L.J., Dong, X.Y., Zhao, M.Q., Shen, H.Y., Wang, J.Y., Pei, J.J., Liu, W.J., Luo, Y.W., Ju, C.M., Chen, J.D., 2012b. Classical swine fever virus failed to activate nuclear factor-kappa B signaling pathway both in vitro and in vivo. *Virol. J.* 9, 293.
- Cole, J.L., 2007. Activation of PKR: an open and shut case? *Trends Biochem. Sci.* 32 (2), 57–62.
- Diaz, D.A.H., Nunez, J.I., Ganges, L., Barreras, M., Frias, M.T., Sobrino, F., 1998. An RT-PCR assay for the specific detection of classical swine fever virus in clinical samples. *Vet. Res.* 29 (5), 431–440.
- Elbahesh, H., Scherbik, S.V., Brinton, M.A., 2011. West Nile virus infection does not induce PKR activation in rodent cells. *Virology* 421, 51–60.
- Fletcher, S.P., Jackson, R.J., 2002. Pestivirus internal ribosome entry site (IRES) structure and function: elements in the 5' untranslated region important for IRES function. *J. Virol.* 76 (10), 5024–5033.
- Friis, M.B., Rasmussen, T.B., Belsham, G.J., 2012. Modulation of translation initiation efficiency in classical swine fever virus. *J. Virol.* 86 (16), 8681–8692.
- Gale, M.J., Blakely, C.M., Kwieciszewski, B., Tan, S.L., Dossett, M., Tang, N.M., Korth, M.J., Polyak, S.J., Gretch, D.R., Katze, M.G., 1998. Control of PKR protein kinase by hepatitis C virus nonstructural 5A protein: molecular mechanisms of kinase regulation. *Mol. Cell. Biol.* 18 (9), 5208–5218.
- Garcia, M.A., Gil, J., Ventoso, I., Guerra, S., Domingo, E., Rivas, C., Esteban, M., 2006. Impact of protein kinase PKR in cell biology: from antiviral to antiproliferative action. *Microbiol. Mol. Biol. Rev.* 70 (4), 1032–1060.
- Gil, J., Alcamí, J., Esteban, M., 1999. Induction of apoptosis by double-stranded-RNA-dependent protein kinase (PKR) involves the alpha subunit of eukaryotic translation initiation factor 2 and NF-kappaB. *Mol. Cell. Biol.* 19 (7), 4653–4663.
- Hashem, Y., des Georges, A., Dhote, V., Langlois, R., Liao, H.Y., Grassucci, R.A., Pestova, T.V., Hellen, C.U., Frank, J., 2013. Hepatitis-C-virus-like internal ribosome entry sites displace eIF3 to gain access to the 40S subunit. *Nature* 503 (7477), 539–543.
- He, B., Gross, M., Roizman, B., 1997. The gamma(1)34.5 protein of herpes simplex virus 1 complexes with protein phosphatase 1alpha to dephosphorylate the alpha subunit of the eukaryotic translation initiation factor 2 and preclude the shutoff of protein synthesis by double-stranded RNA-activated protein kinase. *Proc. Natl. Acad. Sci. U. S. A.* 94 (3), 843–848.
- He, D.N., Zhang, X.M., Liu, K., Pang, R., Zhao, J., Zhou, B., Chen, P.Y., 2014. In vitro inhibition of the replication of classical swine fever virus by porcine Mx1 protein. *Antiviral Res.* 104, 128–135.
- He, Y., Tan, S.L., Tareen, S.U., Vijaysri, S., Langland, J.O., Jacobs, B.L., Katze, M.G., 2001. Regulation of mRNA translation and cellular signaling by hepatitis C virus nonstructural protein NSSA. *J. Virol.* 75 (11), 5090–5098.
- Hsu, W.L., Chen, C.L., Huang, S.W., Wu, C.C., Chen, I.H., Nadar, M., Su, Y.P., Tsai, C.H., 2014. The untranslated regions of classic swine fever virus RNA trigger apoptosis. *PLOS ONE* 9 (2), e88863.
- Hu, Y., Conway, T.W., 1993. 2-Aminopurine inhibits the double-stranded RNA-dependent protein kinase both in vitro and in vivo. *J. Interferon Res.* 13 (5), 323–328.
- Jackson, R.J., Hellen, C.U., Pestova, T.V., 2010. The mechanism of eukaryotic translation initiation and principles of its regulation. *Nat. Rev. Mol. Cell Biol.* 11 (2), 113–127.
- Jiang, D., Weidner, J.M., Qing, M., Pan, X.B., Guo, H., Xu, C., Zhang, X., Birk, A., Chang, J., Shi, P.Y., Block, T.M., Guo, J.T., 2010. Identification of five interferon-induced cellular proteins that inhibit west nile virus and dengue virus infections. *J. Virol.* 84 (16), 8332–8341.
- Kang, R., Tang, D., 2012. PKR-dependent inflammatory signals. *Sci. Signal.* 5 (247), pe47.
- Kang, W., Sung, P.S., Park, S.H., Yoon, S., Chang, D.Y., Kim, S., Han, K.H., Kim, J.K., Rehermann, B., Chwae, Y.J., Shin, E.C., 2014. Hepatitis C virus attenuates interferon-induced major histocompatibility complex class I expression and decreases CD8+ T cell effector functions. *Gastroenterology* 146 (5), 1351–1360 (e1–e4).
- Kedersha, N., Chen, S., Gilks, N., Li, W., Miller, I.J., Stahl, J., Anderson, P., 2002. Evidence that ternary complex (eIF2-GTP-tRNA(i)(Met))-deficient preinitiation complexes are core constituents of mammalian stress granules. *Mol. Biol. Cell* 13 (1), 195–210.
- Knoetig, S.M., McCullough, K.C., Summerfield, A., 2002. Lipopolysaccharide-induced impairment of classical swine fever virus infection in monocytic cells is sensitive to 2-aminopurine. *Antiviral Res.* 53 (1), 75–81.
- Kumar, A., Yang, Y.L., Flati, V., Der, S., Kadereit, S., Deb, A., Haque, J., Reis, L., Weissmann, C., Williams, B.R., 1997. Deficient cytokine signaling in mouse embryo fibroblasts with a targeted deletion in the PKR gene: role of IRF-1 and NF-kappaB. *EMBO J.* 16 (2), 406–416.
- Lindquist, M.E., Mainou, B.A., Dermody, T.S., Crowe, J.J., 2011. Activation of protein kinase R is required for induction of stress granules by respiratory syncytial virus but dispensable for viral replication. *Virology* 413 (1), 103–110.
- Locker, N., Easton, L.E., Lukavsky, P.J., 2007. HCV and CSFV IRES domain II mediate eIF2 release during 80S ribosome assembly. *EMBO J.* 26 (3), 795–805.
- Lopez, S., Arias, C.F., 2012. Rotavirus-host cell interactions: an arms race. *Curr. Opin. Virol.* 2 (4), 389–398.
- Moennig, V., Becher, P., Beer, M., 2013. Classical swine fever. *Dev. Biol. (Basel)* 135, 167–174.
- Nakamura, T., Furuhashi, M., Li, P., Cao, H., Tuncman, G., Sonenberg, N., Gorgun, C.Z., Hotamisligril, G.S.G.H., 2010. Double-stranded RNA-dependent protein kinase links pathogen sensing with stress and metabolic homeostasis. *Cell* 140 (3), 338.
- Noursadeghi, M., Tsang, J., Haustein, T., Miller, R.F., Chain, B.M., Katz, D.R., 2008. Quantitative imaging assay for NF-kappaB nuclear translocation in primary human macrophages. *J. Immunol. Methods* 329 (1–2), 194–200.
- Pei, J., Zhao, M., Ye, Z., Gou, H., Wang, J., Yi, L., Dong, X., Liu, W., Luo, Y., Liao, M., Chen, J., 2014. Autophagy enhances the replication of classical swine fever virus in vitro. *Autophagy* 10 (1), 93–110.
- Perez, L.J., Diaz, D.A.H., Tarradas, J., Rosell, R., Perera, C.L., Munoz, M., Frias, M.T., Nunez, J.I., Ganges, L., 2011. Development and validation of a novel SYBR Green real-time RT-PCR assay for the detection of classical swine fever virus evaluated on different real-time PCR platforms. *J. Virol. Methods* 174 (1–2), 53–59.
- Pestova, T.V., de Breyne, S., Pisarev, A.V., Abaeva, I.S., Hellen, C.U., 2008. eIF2-dependent and eIF2-independent modes of initiation on the CSFV IRES: a common role of domain II. *EMBO J.* 27 (7), 1060–1072.
- Rojas, M., Arias, C.F., Lopez, S.S.I.U., 2010. Protein kinase R is responsible for the phosphorylation of eIF2 alpha in rotavirus infection. *J. Virol.* 84, 10457–10466.
- Ruggli, N., Bird, B.H., Liu, L., Bauhofer, O., Tratschin, J.D., Hofmann, M.A., 2005. N(pro) of classical swine fever virus is an antagonist of double-stranded RNA-mediated apoptosis and IFN-alpha/beta induction. *Virology* 340 (2), 265–276.
- Ruggli, N., Summerfield, A., Fiebach, A.R., Guylack-Pirion, L., Bauhofer, O., Lamm, C.G., Waltersperger, S., Matsuno, K., Liu, L., Gerber, M., Choi, K.H., Hofmann, M.A., Sakoda, Y., Tratschin, J.D., 2009. Classical swine fever virus can remain virulent after specific elimination of the interferon regulatory factor 3-degrading function of N<sup>pro</sup>. *J. Virol.* 83, 817–829.
- Sarnow, P., 2003. Viral internal ribosome entry site elements: novel ribosome-RNA complexes and roles in viral pathogenesis. *J. Virol.* 77 (5), 2801–2806.
- Schneider, R.J., Safer, B., Munemitsu, S.M., Samuel, C.E., Shenk, T., 1985. Adenovirus VAI RNA prevents phosphorylation of the eukaryotic initiation factor 2 alpha subunit subsequent to infection. *Proc. Natl. Acad. Sci. U. S. A.* 82 (13), 4321–4325.
- Seago, J., Goodbourn, S., Charleston, B., 2010. The classical swine fever virus N<sup>pro</sup> product is degraded by cellular proteasomes in a manner that does not require interaction with interferon regulatory factor 3. *J. Gen. Virol.* 91 (Pt 3), 721–726.

- Seago, J., Hilton, L., Reid, E., Doceul, V., Jeyatheesan, J., Moganeradj, K., McCauley, J., Charleston, B., Goodbourn, S., 2007. The Npro product of classical swine fever virus and bovine viral diarrhea virus uses a conserved mechanism to target interferon regulatory factor-3. *J. Gen. Virol.* 88 (Pt 11), 3002–3006.
- Sheng, C., Chen, Y., Xiao, J., Xiao, J., Wang, J., Li, G., Chen, J., Xiao, M., 2012. Classical swine fever virus NS5A protein interacts with 3'-untranslated region and regulates viral RNA synthesis. *Virus Res.* 163 (2), 636–643.
- Silva, A.M., Whitmore, M., Xu, Z., Jiang, Z., Li, X., Williams, B.R., 2004. Protein kinase R (PKR) interacts with and activates mitogen-activated protein kinase kinase 6 (MKK6) in response to double-stranded RNA stimulation. *J. Biol. Chem.* 279 (36), 37670–37676.
- Stewart, M.J., Blum, M.A., Sherry, B., 2003. PKR's protective role in viral myocarditis. *Virology* 314 (1), 92–100.
- Taloczy, Z., Jiang, W., Virgin, H.T., Leib, D.A., Scheuner, D., Kaufman, R.J., Eskelinen, E.L., Levine, B., 2002. Regulation of starvation- and virus-induced autophagy by the eIF2alpha kinase signaling pathway. *Proc. Natl. Acad. Sci. U. S. A.* 99 (1), 190–195.
- Taylor, S.S., Haste, N.M., Ghosh, G., 2005. PKR and eIF2alpha: integration of kinase dimerization, activation, and substrate docking. *Cell* 122 (6), 823–825.
- Tian, B., Mathews, M.B., 2001. Functional characterization of and cooperation between the double-stranded RNA-binding motifs of the protein kinase PKR. *J. Biol. Chem.* 276 (13), 9936–9944.
- Toroney, R., Nallagatla, S.R., Boyer, J.A., Cameron, C.E., Bevilacqua, P.C., 2010. Regulation of PKR by HCV IRES RNA: importance of domain II and NS5A. *J. Mol. Biol.* 400 (3), 393–412.
- Tu, Y.C., Yu, C.Y., Liang, J.J., Lin, E., Liao, C.L., Lin, Y.L., 2012. Blocking double-stranded RNA-activated protein kinase PKR by Japanese encephalitis virus nonstructural protein 2A. *J. Virol.* 86 (19), 10347–10358.
- Wang, X., Liao, Y., Yap, P.L., Png, K.J., Tam, J.P., Liu, D.X., 2009. Inhibition of protein kinase R activation and upregulation of GADD34 expression play a synergistic role in facilitating coronavirus replication by maintaining de novo protein synthesis in virus-infected cells. *J. Virol.* 83 (23), 12462–12472.
- Zhu, J., Carver, W., 2012. Effects of interleukin-33 on cardiac fibroblast gene expression and activity. *Cytokine* 58 (3), 368–379.